

# Analytical Prediction of Crushing Thin-Walled Square Tube with Static Axial Loads Using Elliptical Holes as Crush Initiators

Endarto Tri Wibowo<sup>1,a\*</sup>, Jos Istiyanto<sup>1,b</sup>, Danardono Agus Sumarsono<sup>1,c</sup>,  
Dony Hidayat<sup>1,d</sup>

<sup>1</sup>Department of Mechanical Engineering, Faculty of Engineering, Universitas Indonesia, Kampus UI Depok, Depok 16424, Indonesia

\*Email: <sup>a</sup>enda043@brin.go.id, <sup>b</sup>josist@eng.ui.ac.id, <sup>c</sup>dasumarsono@gmail.com,  
<sup>d</sup>dony.hidayat@brin.go.id

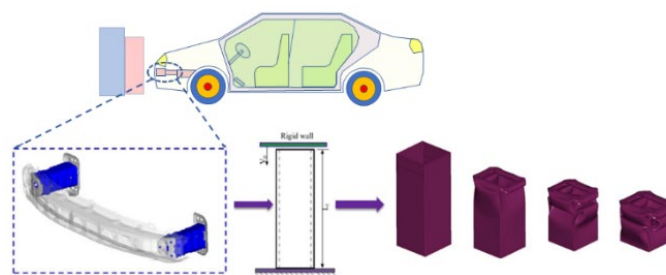
**Keywords:** Impact energy absorber, analytical, square tube, elliptical hole.

**Abstract:** In the structure of passenger vehicles there are components that absorb the impact load, which components are commonly thin-walled square tube. The design of the impact energy absorber model can be carry-out by experiment, simulation, and analysis. In the design of this impact energy absorbing component, an elliptical hole was used as a crush initiator to reduce peak loads and set the start of the bending pattern. Analytical predictions were made to reduce costs and speed up time to obtain mean load and peak loads values from the same shape model. In this study, a thin-walled square tubes model is used with an elliptical hole that have ratio of horizontal axis and vertical axis is from 3:7 until 7:3. The result of this study showed that the prediction of the peak load and average load by analytical means has a good conformity with the simulation.

## 1. Introduction

According to data from the Indonesian Central Statistics Agency (BPS), it was known that there is an increase in the number of vehicles by around 4.8% every year [1]. So, it is very important to have criteria from vehicle design to ensure the safety and security of passengers in the event of an accident / crushes (crashworthiness). Criteria in crashworthiness are important for application in the design of motorized vehicles, cars, buses, trains and ships. Where in the design of the vehicle structure there is a collision energy absorption zone (crumple zone) which functions to protect passengers so that they remain safe in the passenger compartment when a crushing occurs.

Several factors that affect crashworthiness are the absorptive energy value of a structure including the load from the impact force, the crash initiator (trigger from the folding direction), the geometry of the shape of the object, the type of material and the mass of the specimen [2, 3, 4, 5, 6, 22]. The criteria for the impact energy absorption model include energy absorption (EA), specific energy absorption (SEA), mean crushing force (MCF), peak crushing force (PCF), and crushing force efficiency (CFE). The CFE is obtained from a comparison between the MCF and PCF values. The PCF value is expected not too high, this is to avoid serious injury or death of passengers due to the influence of high decelerations toward the limits of the abilities human body if the collision was happened. While SEA is obtained from the comparison between the EA value and the mass of the material [7].



**Fig. 1.** Location of the component structure for energy absorption / *crashworthiness* of the vehicle [8].

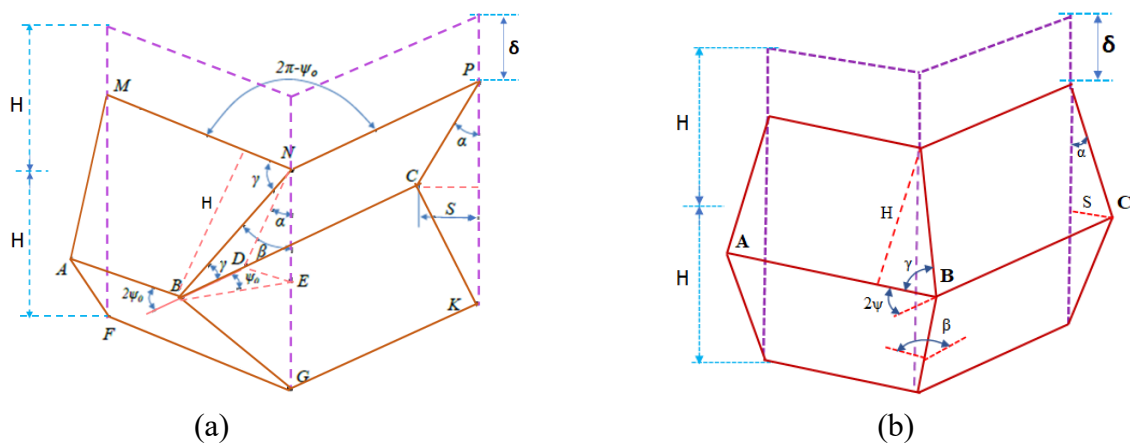
In the process of analysing energy absorption in structures, which can commonly be carried out analytically, numerical simulations, and validation processes with experiments. Where on the experiment need specimen or test objects, sensors, and equipment that do not slightly, while in the simulation possible more a little equipment, however still need a computer with specification high specific and also analysis software collisions (ANSYS LS-DYNA, ABAQUS, and Pam Crash), where both of methods require significant costs. So that analytical calculations were developed to make it easier in calculating the predictions on the estimated value of the mean load and peak load when the crushing occurs. This will be faster because the calculation time is relatively fast with the equations that have been made and it is easier with less resource requirements.

In this paper, analytical prediction was developed on the mean load and peak load calculation when the static axial impact loads occur in a thin-walled square tube with an elliptical hole. Where is the elliptical hole as the crush initiator and controls when the first bending occurs. The elliptical hole consists of a major axis in horizontal position (a) and a minor axis in vertical position (b), with variations in the size ratio (a/b) that influencing the load impact values. After the results of the analytical calculations are obtained, then comparing with the simulation to show trend of result.

## 2. Materials and Methods

In predicting the energy absorption value of static axial load on thin-walled square tube by analytical calculations, it has started from the basic folding mechanism method presented by Abramowicz and Wierbicki [10]. Where in modeling the buckling deformation in general there are 2 types of buckling models, namely inextensional collapse modes (mode I) and extensional collapse mode (II) [11].

In the deformation of modes I for simplifying the calculation amount of energy absorption rate in terms of the basic folding mechanism in movement of the bent deformation on the square tube there are 3 different mechanism parts, namely the energy rate on the surface part of the toroidal ( $E_1$ ), the energy rate in the horizontal bending line ( $E_2$ ), and energy rate in the inclination bending line ( $E_3$ ) [9, 10]. As for the extensional deformation (mode II) in calculating values of the energy absorption rate from the bending deformation motion, there are also 3 different mechanisms, namely the energy rate on the trapezoidal surface ( $E_4$ ), the energy rate on the horizontal bending line ( $E_5$ ), and energy rate at the inclination bending line ( $E_6$ ) [11,13].



**Fig. 2.** Basic folding mechanism, (a). inextensional collapse modes (Mode I) [10,19] (b). extensional collapse mode (Mode II) [13].

When the collision occurs, there will be deformation in the form of bending on the surface of the energy absorbing structure. This bending causes a change in length ( $\delta$ ) before and after the collision, as well as a change in angle ( $\alpha$ ). Referring to **Fig. 2.a** and **2.b**, the relationship between the distance of the change in length ( $\delta$ ) and the change in angle ( $\alpha$ ) is as follows:

$$\delta = 2H (1 - \cos \alpha) \quad \text{..... (1)}$$

Where,  $H$  is a half wavelength of the bending, from Eq.1 it can be seen that when  $\alpha = 0^\circ$  then ( $\cos 0^\circ = 1$ ); which means  $\delta = 0$  (no folds yet), while at  $\alpha = 90^\circ$  ( $\cos 90^\circ = 0$ ); means  $\delta = 2H$  (maximum fold). Meanwhile, the value of the horizontal displacement distance ( $s$ ) at point C (**Fig. 2**), is:

$$s = H \sin \alpha \quad \text{..... (2)}$$

Then from Eq.1 it can be derived to be the axial motion velocity ( $\dot{\delta}$ ), with the following Eq.:

$$\dot{\delta} = 2H (\sin \alpha) \dot{\alpha} \quad \text{..... (3)}$$

Meanwhile, from Eq.2 it is derived to be the horizontal velocity ( $\dot{s}$ ), with the following Eq.:

$$v = \dot{s} = H (\cos \alpha) \dot{\alpha} \quad \text{..... (4)}$$

For the relationship between corner  $\alpha$ ,  $\beta$ ,  $\gamma$ ,  $\psi_0$ , referring to the type of mode I in **Fig. 2.a**, are as following [9][19].

$$\tan \gamma = \frac{\tan \psi_0}{\sin \alpha}; \tan \beta = \frac{\tan \alpha}{\sin \psi_0} \quad \text{..... (5)}$$

Where  $\angle \psi_0 = \text{EBD}$ ;  $\angle \alpha = \text{END}$ ;  $\angle \beta = \text{ENB}$ ;  $\angle \gamma = \text{DBN}$

In the inextensional deformation type (mode I) for the equation of the energy absorption rate consist of 3 constituent parts [9,10,12], that is,

a. The energy dissipation rate on the toroidal surface ( $E_1$ ), with the following Eq.:

$$E_1 = 4N_0 H b I_1 = 16 M_0 \cdot \frac{H \cdot b}{h} I_1 \quad \text{..... (6)}$$

With Eq.  $I_1$  is,

$$I_1 = \frac{\pi}{(\pi - 2\psi_0) \tan \psi_0} \cdot \int_0^{\pi/2} \cos \alpha \left\{ \cos \psi_0 - \cos \left( \psi_0 + \frac{\pi - 2\psi_0}{\pi} \beta \right) \right\} d\alpha \quad \text{..... (6a)}$$

Where,  $I_1$  is integral value on the toroidal section;  $N_0$  is fully plastic membrane force;  $M_0$  is fully plastic bending moment;  $b$  is the small radius from toroidal surface.

b. The energy dissipation rate on the horizontal bending line ( $E_2$ ), with the following Eq.:

$$E_2 = \frac{1}{2} M_0 C \pi \quad \text{..... (7)}$$

Where,  $C$  is length of the horizontal bending line.

c. The energy dissipation rate at the inclination bending line ( $E_3$ ), the Equation is.

$$E_3 = 4 M_0 \frac{H^2}{b} I_3 \quad \text{..... (8)}$$

Where  $I_3$  is,

$$I_3 = \frac{1}{\tan \psi_0} \int_0^{\pi/2} \frac{\cos \alpha}{\sin \gamma} d\alpha \quad \text{..... (8a)}$$

## 2.1 Equation for calculating the internal energy absorption of a basic folding element in a square tube without holes.

According from reference [11], the absorption energies consist of type I and type II on the square tube, respectively,

$$E_{\text{typeI}} = M_0 \left( 16 H \frac{b}{h} I_1 + 2 \pi C + 4 \frac{H^2}{b} I_3 \right) \quad \text{..... (12.a)}$$

$$E_{\text{typeII}} = M_0 \left( 8 \frac{H^2}{h} + 2 \pi C + 4H \right) \quad \text{..... (12.b)}$$

While from reference [10,18] for the average load ( $P_{\text{mean}}$ ) and peak load ( $P_{\text{peak}}$ ) of the square tube without holes, respectively, are

$$P_{\text{mean}} = 9.56 \sigma_0 h^{5/3} C^{1/3} \quad \text{..... (13.a)}$$

$$P_{\text{peak}} = 2,19 K_G \sigma_0 h^{5/3} C^{1/3} \quad \dots (13.b)$$

Where  $K_G$  is geometry coefficient, for square tube without hole is 16,41.

## 2.2 Energy calculation of the horizontal hinge line on a square tube with 2 elliptical holes on opposite sides.

The existence of a hole will influence the amount of absorption energy in mode I, where the effect of a round hole on a square tube has been calculated [18, 19]. While here it is studied for the influence of elliptical holes on 2 opposite sides which affect the horizontal hinge line, with the following calculations:

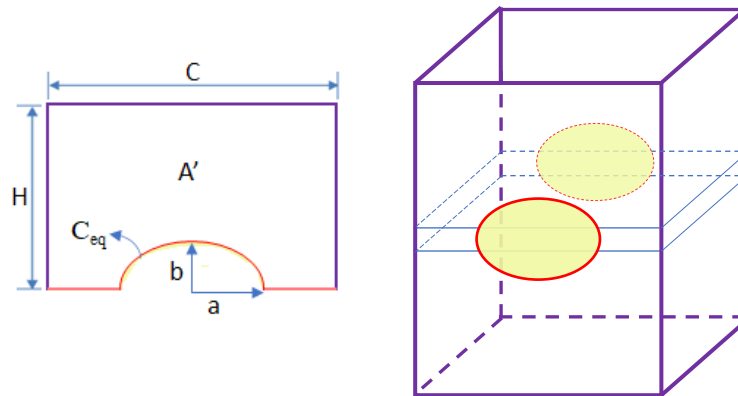


Fig. 3. Geometry model with elliptical holes on square tube.

From **Fig. 3** it can be seen that the length of the horizontal line is  $C$ , while the horizontal line with the elliptical hole is  $C_{eq}$ , for  $A$  is the area of the field without the elliptical hole,  $A'$  is the area of the field with the elliptical hole, and  $a$  is the distance of the horizontal axis on the ellipse, and  $b$  is distance of the vertical axis on the ellipse, so the equation is obtained,

$$\begin{aligned} \frac{C_{eq}}{C} &= \frac{A'}{A} = \frac{A - \frac{\pi \cdot a \cdot b}{2}}{A} = 1 - \frac{\pi \cdot a \cdot b}{2A} = 1 - \frac{\pi \cdot a \cdot b}{2CH} \\ C_{eq} &= \left(1 - \frac{\pi \cdot a \cdot b}{2CH}\right)C \end{aligned} \quad \dots (14)$$

There is an influence of the elliptical shape factor on the ratio of the length between the vertical axis and the horizontal axis when the collision occurs, which influence the magnitude of the peak load value as stated in reference [21]. So that the ratio of the length of the vertical axis to the horizontal becomes a coefficient.

In this study to determine the coefficient of an elliptical shape similar with a circle, where the calculation of area of the circle is influenced by the dimension  $r$  (radius) while for the ellipse it is influenced by the dimensions  $a$  (major axis) and  $b$  (minor axis). So that  $r$  square is equivalent to a times  $b$ . When viewed from the calculation of the circumference, the circle is influenced by the diameter ( $2r$ ) while for the ellipse the size of the circumference is influenced by the summation of  $a$  and  $b$ . The equation is as follows,

Area of circle  $\approx$  Area of ellipse

$$\pi \cdot r^2 \approx \pi \cdot a \cdot b$$

$$\text{so } \rightarrow r^2 \approx a \cdot b$$

$$\text{can written too } \rightarrow r_1 \cdot r_2 \approx a \cdot b$$

Circumference of the circle  $\approx$  Circumference of the ellipse

$$\pi \cdot 2r \approx \pi \cdot (a + b)$$

$$\text{can written too } \rightarrow r_1 + r_2 \approx a + b$$

$$\text{If, } r_1 = r_2 = r \rightarrow \text{so, } a + b \approx 2r$$

$$2r = a + b$$

$$r = \frac{a + b}{2}$$

$$r^2 = \left(\frac{a+b}{2}\right)^2$$

$$r^2 = \frac{(a+b)^2}{2^2}$$

The quantity Area of circle  $\approx$  Area of ellipse  $\rightarrow$  when is given constant multiplier, is obtained

$$k. \pi. r^2 = \pi. \frac{(a+b)^2}{2^2} \rightarrow \text{If, } r^2 = 1$$

$$k = \frac{(a+b)^2}{2^2} = \frac{a^2 + 2ab + b^2}{2^2}. \quad \dots (15)$$

Where according on reference data [21] it is known that the influence of dimensions of the horizontal axis (a) is about 10 times greater than the vertical axis (b) for the result of peak loads. By using the weighting coefficient on the values of a and b, where a = 0.1 and b = 0.01. So, the coefficient a is different with b. Another effect for the elliptical hole on 1 side is related to the energy dissipation with the horizontal hinge line effect is 2/16 or 1/8. To estimate the elliptical shape coefficient (k) is as follows:

$$k = \frac{(0,1a^2 + 0,01b)^2}{2^2.8} \quad \dots (15.a)$$

Then, the effect of  $C_{eq}$  for the energy rate dissipation ( $\dot{E}_2$ ) on the horizontal hinge line with the condition of 2 elliptical holes on the opposite sides, so that the value of  $\dot{E}_2$  on the square tube is composed of 12 horizontal hinge lines C and 4 horizontal hinge lines  $C_{eq}$ . So, the following equation is obtained:

$$\dot{E}_2 = 12.M_0. C. \dot{\alpha} + 4. M_0. C_{eq}. \dot{\alpha} \quad \dots (16.a)$$

Simplified to be,

$$\dot{E}_2 = 4. M_0. (3C + C_{eq}). \dot{\alpha} \quad \dots (16.b)$$

By substituting Eq.14 into Eq.16.b, we get,

$$\dot{E}_2 = 4. M_0. (3C + (1 - \frac{\pi. a. b}{2CH})C) \dot{\alpha} \quad \dots (17.a)$$

$$\dot{E}_2 = 4. M_0. (4 - \frac{\pi. a. b}{2CH}). C \dot{\alpha} \quad \dots (17.b)$$

Where the value of  $\dot{\alpha}$  is from 0 to  $\frac{\pi}{2}$ , so when integrated, the energy dissipation value obtained is,

$$E_2 = 4. M_0. (4 - \frac{\pi. a. b}{2CH}). C \int_0^{\pi/2} d\alpha \quad \dots (18.a)$$

$$E_2 = 2. M_0. \pi. (4 - \frac{\pi. a. b}{2CH}). C \quad \dots (18.b)$$

$$E_2 = M_0. \pi. (8 - \frac{\pi. a. b}{CH}). C \quad \dots (18.c)$$

### 2.3 Symmetric collapse mode with 2 elliptical holes on opposite sides.

For calculation of the mean load ( $P_m$ ) from the absorption energy in symmetric collapse mode where the external energy balance is equal to the internal energy, so the external energy value is 4 times energy of type I [10, 11]. So, the absorption energy equation for symmetric collapse on a square tube with 2 elliptical holes is obtained, by the following equation is,

$$E_{ext} = 4 E_{type I} \quad \dots (19.a)$$

$$E_{ext} = P_m. 2H \quad \dots (19.b)$$

$$P_m. 2H = 4 E_1 + E_2 + 4 E_3 \quad \dots (19.c)$$

By substitution Eq.6, 18.c, and 8 into Eq.19.c, hence the result,

$$P_m \cdot 2H = M_0 \left[ 64 I_1 \cdot H \cdot \left( \frac{b}{h} \right) + \pi \cdot \left( 8 - \frac{\pi \cdot a \cdot b}{CH} \right) \cdot C + 16 \cdot I_3 \cdot \frac{H^2}{b} \right] \quad \text{..... (20.a)}$$

$$\frac{P_m}{M_0} = 32 I_1 \cdot \left( \frac{b}{h} \right) + \left[ 4 - \frac{\pi \cdot a \cdot b}{2CH} \right] \pi \cdot \left( \frac{C}{H} \right) + 8 \cdot I_3 \cdot \left( \frac{H}{b} \right) \quad \text{..... (20.b)}$$

If,  $A_1 = 32 I_1$  ;  $A_2 = \pi \left[ 4 - \frac{\pi \cdot a \cdot b}{2CH} \right]$  ;  $A_3 = 8 I_3$

The Eq.20.b can be simplified with these coefficients. So, the following form of the equation is obtained, namely,

$$\frac{P_m}{M_0} = A_1 \cdot \left( \frac{b}{h} \right) + A_2 \cdot \left( \frac{C}{H} \right) + A_3 \cdot \left( \frac{H}{b} \right) \quad \text{..... (21)}$$

Where according to reference [10] for a square tube ( $\psi_0 = \pi/4$ ), the value of  $I_1 = 0.58$ , and  $I_3 = 1.11$  are obtained. Whereas for,

$$\left( \frac{b}{h} \right) = 0.72 \left( \frac{C}{h} \right)^{1/3} \quad \text{..... (22.a)}$$

$$H = 0.983 \sqrt[3]{C^2 h} \quad \text{..... (22.b)}$$

$$b = 0.687 \sqrt[3]{C h^2} \quad \text{..... (22.c)}$$

By substituting the values  $A_1$ ,  $A_2$ , and  $A_3$  with Eq.22a, 22b, and 22c into Eq.21, so the following equation is obtained,

$$\frac{P_m}{M_0} = (26.05) \cdot \left( \frac{C}{h} \right)^{1/3} + \left( \pi \cdot \left[ 4 - \frac{\pi \cdot a \cdot b}{2CH} \right] \right) (1.02) \left( \frac{C}{h} \right)^{1/3} \quad \text{..... (23)}$$

It's known that  $M_0 = \frac{1}{4} \sigma_0 h^2$ , then the value of the mean force ( $P_m$ ) is

$$P_m = \sigma_0 \left[ (6.513) \cdot C^{1/3} \cdot h^{5/3} + \left( \left[ 4 - \frac{\pi \cdot a \cdot b}{2CH} \right] \pi \right) \cdot (0.255) \cdot C^{1/3} \cdot h^{5/3} \right] \quad \text{..... (24)}$$

Based on reference [11] for the effective crushing distance ( $\delta$ ) in symmetric collapse mode, is

$$0.73 = \frac{\delta}{2H} \quad \text{..... (25)}$$

By dividing Eq.24 by Eq.25 and inserting the effect of the ellipse shape coefficient ( $k$ ) from Eq.15a, so the value of mean static force ( $\bar{P}_{\text{mean}}$ ) is,

$$\bar{P}_{\text{mean}} = \sigma_0 \left[ (8.922) \cdot C^{1/3} \cdot h^{5/3} + \left( \left[ 4 - \frac{\pi \cdot a \cdot b}{2CH} \right] \pi \right) \cdot k \cdot (0.349) \cdot C^{1/3} \cdot h^{5/3} \right] \quad \text{..... (26)}$$

The peak crushing force is the instantaneous peak value at the collision, with a value above of the mean static force ( $\bar{P}_{\text{mean}}$ ) so it is necessary to have a peak collision force coefficient ( $K_0$ ), and geometry coefficient ( $K_G$ ) where from reference [18] the value of  $K_0 = 2.19$ . So that is obtained,

$$\bar{P}_{\text{peak}} = 2.19 \cdot K_G \cdot \bar{P}_{\text{mean}}$$

$$\bar{P}_{\text{peak}} = 2.19 \cdot K_G \cdot \sigma_0 \left[ (8.922) \cdot C^{1/3} \cdot h^{5/3} + \left( \left[ 4 - \frac{\pi \cdot a \cdot b}{2CH} \right] \pi \right) \cdot k \cdot (0.349) \cdot C^{1/3} \cdot h^{5/3} \right] \quad \text{..... (27)}$$

Based on reference [18] for the calculation of  $K_G$  is

$$K_G = \frac{3}{4} \sqrt[3]{A_1 \cdot A_2 \cdot A_3} \quad \text{..... (28)}$$

For the values  $A_1$  and  $A_3$  related to the value of the  $\alpha_{\text{peak}}$  angle when peak crushing was occur. So, the equation is

$$A_1 = 32 \sqrt{2} \cdot \cot \alpha_{peak} \cdot \left[ \left( \sqrt{\frac{1}{2} - \frac{1}{2 \sqrt{2 \tan^2 \alpha_{peak} + 1}}} \right) - \left( \sqrt{\frac{1}{2} + \frac{1}{2 \sqrt{2 \tan^2 \alpha_{peak} + 1}}} \right) + 1 \right] \quad \dots (29.a)$$

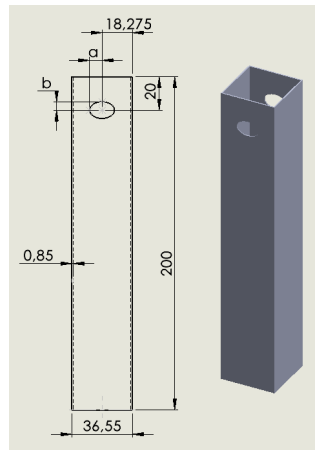
$$A_3 = 8 \cot \alpha_{peak} \cdot \sqrt{1 + \sin^2 \alpha_{peak}} \quad \dots (29.b)$$

Whereas for  $A_2$  it is influenced by the value of  $E_2$  on the horizontal hinge line and also the influence of elliptical shape was affecting the weight values on  $a$  and  $b$ . so we get the equation,

$$A_2 = (0.001) \frac{\left( 8 - \frac{\pi \cdot a \cdot b}{CH} \right)}{\sin \alpha_{peak}} \quad \dots (29.c)$$

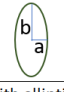
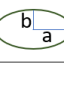
## 2.4 Size and dimensions of models

As for size of the model specimen was based on reference [20]. With a square tube cross section size is 36.55 mm x 36.55 mm; Side width (C) is 36.55mm; square tube wall thickness (h) is 0.85 mm; the total length of the specimen model (L) is 200 mm. Then in this study using 2 ellipse holes which are located on 2 opposite sides with the distance between the center point of the ellipse and the tip (H) is 20 mm, for illustration can be seen in **Fig.4**. While shape of the elliptical hole is made with varying sizes on the horizontal axis ( $a$ ) and the vertical axis ( $b$ ) with sizes shown in **Table 1**.



**Fig.4.** Size of square tube with crush initiator.

**Table 1.** Size variation of the horizontal and vertical axis on the elliptical holes.

No	Specimen models	Size of axis		Ratio a/b	Size of area [mm <sup>2</sup> ]
		Horizontal axis (a) [mm]	Vertical axis (b) [mm]		
1	Square tube without holes			0	0
2	With elliptical holes a<b 	3:7	3	0.43	65.94
3		4:6	4	0.67	75.36
4		5:7.5	5	0.67	117.75
5		5:6	5	0.83	94.2
7	With elliptical holes a>b 	6:5	6	1.20	94.2
8		6:4	6	1.50	75.36
9		7.5:5	7.5	1.50	117.75
10		7:3	7	2.33	65.94

## 2.5 Simulation with the Finite Element method

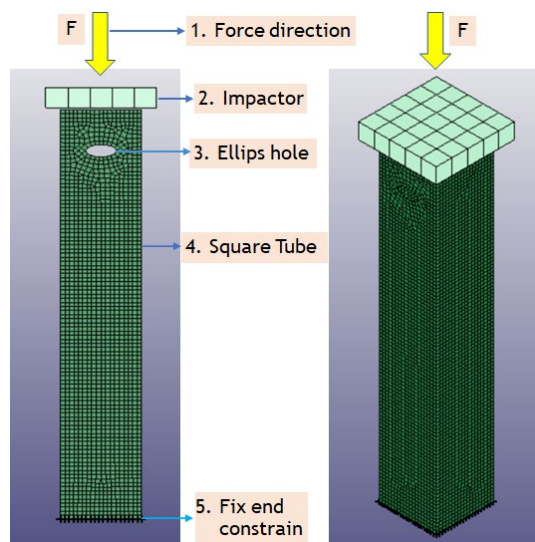
In this study the analytical results were compared with the simulation results obtained from the LS-Dyna software. A thin-walled square tube model was created in the LS-Dyna software with the size and dimensions as previously described (section 2.4). The crushing simulation model consists of

2 components, namely a thin-walled square tube as a specimen model and the beam model as an impactor.

Setting of a thin-walled square tube model for mesh of the wall column using Belytschko-Lin-Tsay-4-nodes with a mesh size of 2x2 mm, it gives optimal and convergence results, so the phenomenon of plastic deformation in the form of indentation in the square tube wall during crash can be properly simulated. In material behaviour a piecewise linear plasticity model is used. As for its material properties are Young's modulus ( $E$ ) is 195 GPa, density( $\rho$ ) is 7850 kg/m<sup>3</sup>, and the value of yield stress ( $\sigma_y$ ) is 265 Mpa [20].

Boundary condition at the bottom end of the square tube is set in fix, there is no displacement ( $x=0$ ,  $y=0$ , and  $z=0$ ). While the direction of impactor movement is only in the downward  $Z$  direction ( $x=0$ ,  $y=0$ , and  $z=-1$ ). Loading is given by the impactor with a constant speed of 0.5 mm/second in line with the axis of the square tube. This condition in static axial loading simulation. For illustration can be seen in **Fig.5**.

As for the impactor beam model, it is made more rigid than square tube, for material type using rigid bodies models. The relation between the surface of square tube and the impactor uses an automatic node to surface contact, where this type of contact prevents penetration and sliding between the impactor wall and the square tube when loading contact occurs. The internal surface relations on the square tube uses automatic-single-surface-contact where this type of contact prevents penetration from between the indentation of square tubes wall when progressive buckling occurs [21].



**Fig. 5.** Loading model with an impactor on a square tube.

### 3. Results and Discussion

#### 3.1 The comparing results between simulation and analytical calculations of square tube without hole.

In the first row of **Table 2** and **Table 3** is a comparison between analytical and simulation results of a square tube without hole. For the average force ( $P_{\text{mean}}$ ) of analytical calculation is obtained 7944.07 N, while at the peak load ( $P_{\text{peak}}$ ) is 29863.29N, where for  $P_{\text{mean}}$  and  $P_{\text{peak}}$  when compared to the simulation there have deviation 0,9% and 0.3% respectively. While the peak load ( $P_{\text{peak}}$ ) of simulation is 29942 N, when compared to the experimental results on reference [20] there is a difference of 2.7%.

#### 3.2 The comparing results between simulation and analytical calculations of square tube with elliptical holes.


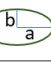
For analytical calculations of the peak load ( $P_{\text{peak}}$ ) on square tube with elliptical holes, the angle value of  $\alpha_{\text{peak}}$  is 23.38° according to reference [18], the calculation results are obtained as follows in **Table 2** and **Table 3**. Analytical calculations have been carried out on several elliptical size variations



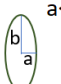
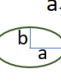
of the ratio 3:7, 4:6, 5:7.5, 5:6, 6:5, 6:4, 7.5:5, 7:3. The results of the comparison between the simulation and analytical values for the average load ( $P_{\text{mean}}$ ) of several elliptical hole size models obtained an average difference of about 3.02% with a range between 0.9% to 5 %. The  $P_{\text{mean}}$  result as in the **Table 2**. While the comparing results for the peak load ( $P_{\text{peak}}$ ) between the simulation and analytical calculation of several elliptical hole size models obtained an average difference of about 3.4% with a range between 0.3% to 9.4%. The  $P_{\text{peak}}$  result as in the **Table 3**.

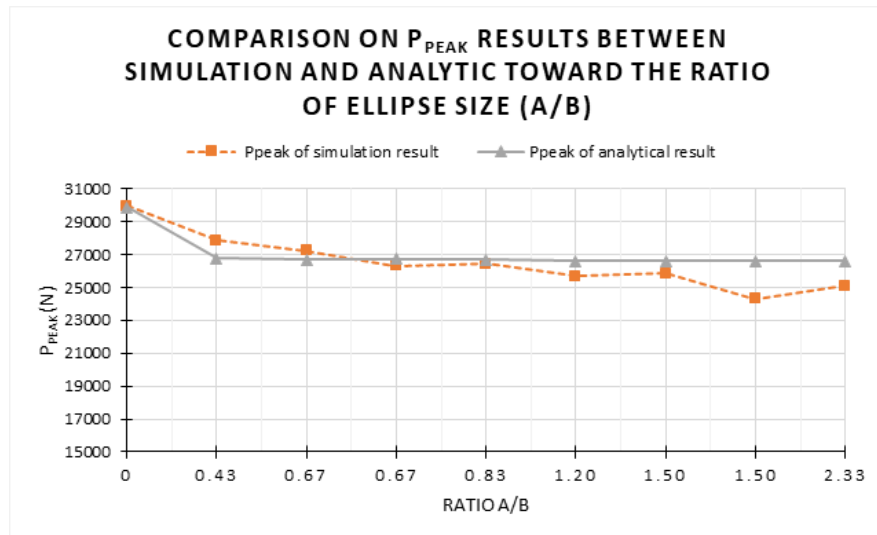
The graph of **Fig. 6** shows the influence the ratio of elliptical holes size on the peak load value. The highest  $P_{\text{peak}}$  value is on a square tube without holes or the ratio  $a/b$  is zero, both by simulation and analytical calculations, namely 29942 N and 29863.3 N respectively, (for detailed numbers in **Table 3**). The lowest  $P_{\text{peak}}$  value is in an elliptical shape with a ratio of 1.5 with a size of 7.5:5 ( $a>b$ ) with simulated and analytical values is 24303 N and 26592.93 N respectively. So that from graph of **Fig. 6** showed that the greater ratio  $a/b$  of the elliptical holes, the trend of peak load ( $P_{\text{peak}}$ ) value will be decrease. The square tube with elliptical holes size  $a<b$  or the ratio  $a/b$  less than 1, the  $P_{\text{peak}}$  values is higher than with elliptical holes size  $a>b$ .

**Table 2.** The comparing results between simulation and analytical calculations on the  $P_{\text{mean}}$  values.

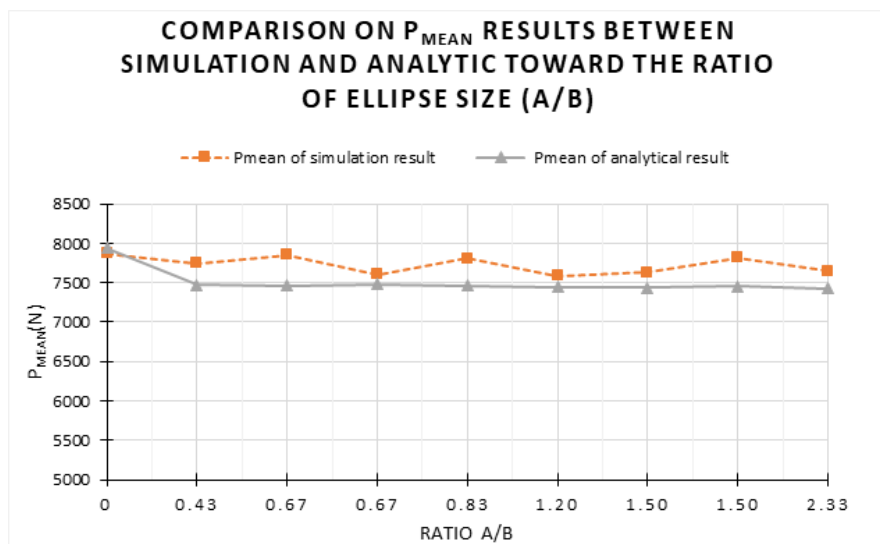
No	Specimen models a:b		Size of axis		Ratio a/b	Size of area Ellips [mm <sup>2</sup> ]	P <sub>mean</sub> Values		deviation [N]	% deviation
			Dimension of Horizontal axis (a) [mm]	Dimension of Vertical axis (b) [mm]			Simulation [N]	Analytics [N]		
1	Square Tube		without holes		0	0	7871	7944.07	73.07	0.9%
2	 a<b	3:7	3	7	0.43	65.94	7744	7473.88	270.12	3.5%
3		4:6	4	6	0.67	75.36	7849	7459.93	389.07	5.0%
4		5:7,5	5	7.5	0.67	117.75	7608	7485.29	122.71	1.6%
5		5:6	5	6	0.83	94.2	7805	7461.23	343.77	4.4%
6	 a>b	6:5	6	5	1.20	94.2	7585	7449.03	135.97	1.8%
7		6:4	6	4	1.50	75.36	7631	7437.68	193.32	2.5%
8		7.5:5	7.5	5	1.50	117.75	7814	7450.78	363.22	4.6%
9		7:3	7	3	2.33	65.94	7646	7429.32	216.68	2.8%
							Average			3.02%

**Table 3.** The comparing results between simulation and analytical calculations on the  $P_{\text{peak}}$  values.

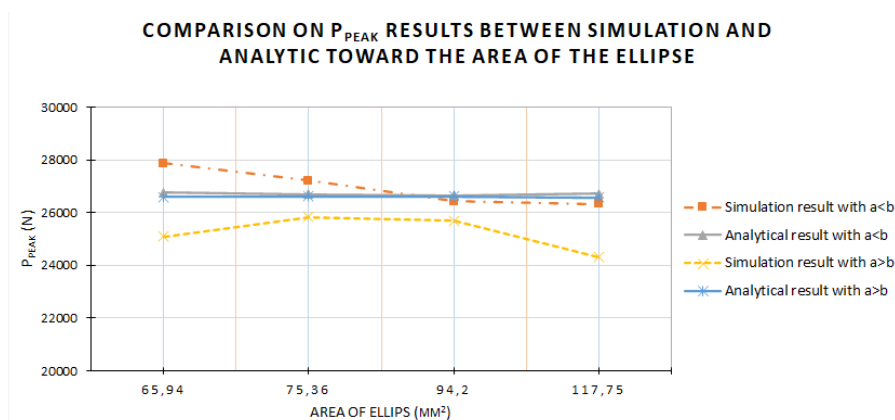
No	Specimen models a:b		Size of axis		Ratio a/b	Size of area Ellips [mm <sup>2</sup> ]	P <sub>peak</sub> Values		deviation [N]	% deviation
			Dimension of Horizontal axis (a) [mm]	Dimension of Vertical axis (b) [mm]			Simulation [N]	Analytics [N]		
1	Square Tube		without holes		0	0	29942	29863.3	78.71	0.3%
2	<div>With elliptical holes</div> <div>a&lt;b</div> 	3:7	3	7	0.43	65.94	27878	26755.52	1122.48	4.0%
3		4:6	4	6	0.67	75.36	27223	26691.07	531.93	2.0%
4		5:7,5	5	7.5	0.67	117.75	26329	26716.09	387.09	1.5%
5		5:6	5	6	0.83	94.2	26435	26666.62	231.62	0.9%
6	<div>With elliptical holes</div> <div>a&gt;b</div> 	6:5	6	5	1.20	94.2	25698	26623.03	925.03	3.6%
7		6:4	6	4	1.50	75.36	25841	26611.47	770.47	3.0%
8		7.5:5	7.5	5	1.50	117.75	24303	26592.93	2289.93	9.4%
9		7:3	7	3	2.33	65.94	25093	26595.98	1502.98	6.0%
							Average			3.40%



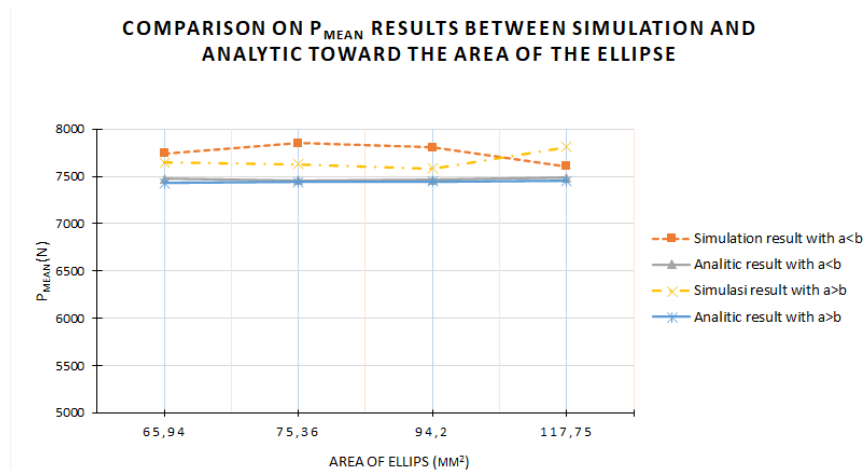
**Fig. 6.** Graph of comparison on  $P_{peak}$  results between simulation and analytic toward the ratio of ellipse size (a/b).



**Fig. 7.** Graph of comparison on  $P_{mean}$  results between simulation and analytic toward the ratio of ellipse size (a/b).



**Fig. 8.** Graph of comparison on  $P_{peak}$  results between simulation and analytic toward the area of the ellipse.



**Fig. 9.** Graph of comparison on  $P_{mean}$  results between simulation and analytic toward the area of the ellipse.

The graph of **Fig. 7** shows the effect of the ratio ( $a/b$ ) at elliptical hole toward the average load. For the highest  $P_{mean}$  value in the square tube without holes both in simulation and analytical calculations, namely 7871 N and 7944.07 N, respectively (for detailed numbers in **Table 2**). The lowest  $P_{mean}$  value for a square tube with elliptical holes at the ratio  $a>b$  where in the simulation at a ratio of 6:5 is 7585 N, while in the analytic calculation at a ratio of 7:3 is 7429.32 N. On the simulation graph the difference between the highest and lowest values is 286 N or 3.6%, while on the analytical chart the difference between the highest and lowest values is 514,75 N or 6.5%. So that the presence of holes can reduce the  $P_{mean}$  value. Meanwhile, the ratio  $a/b$  have relatively small effect on the average load value.

The graph from **Fig. 8** and 9 showed the  $P_{peak}$  and the  $P_{mean}$  value, respectively consists of 4 types of graphs that shows the comparing of the results by simulation and analytic, each consisting of elliptical ratio  $a<b$  and  $a>b$ . The graph of **Fig. 8** showed the effect of the elliptical area size on the peak load. The highest  $P_{peak}$  value is in an elliptical shape with a size ratio  $a<b$  (3:7) with an area of 65.94 mm<sup>2</sup>, namely the simulation results are 27878N, while the analytical results are 26755.52 N (for detailed number in **Table 3**). The lowest value for  $P_{peak}$  on an ellipse with a size ratio  $a>b$  (7.5:5) with an area of 117.75 mm<sup>2</sup>, namely the simulation results are 24303N, while the analytical results are 26592.93 N. On the simulation graph the difference between the highest and lowest values is 3575 N, from this value there is a significant difference, while on the analytical chart the difference between the highest and lowest values is 162.59 N. So that from graph of **Fig. 8** showed that the influence of the area in elliptical hole with the size orientation  $a>b$  toward the  $P_{peak}$  values, where the wider of the elliptical area, so the  $P_{peak}$  value to be lower.

The graph of **Fig. 9** shows the effect of the size of the elliptical area on the average load. For the highest  $P_{mean}$  value from the simulation results is on elliptical shape with a size ratio  $a<b$  (4:6) with an area of 75.36 mm<sup>2</sup> the value is 7849 N, while the lowest value is in elliptical size ratio  $a>b$  (6:5) with an area of 94.2 mm<sup>2</sup> the value is 7585 N, for the difference between the highest and lowest values is 264 N or 3.4%, (for detailed numbers in **Table 2**). For analytical calculations the highest  $P_{mean}$  results are in elliptical shapes with a size ratio  $a<b$  (5:7.5) with an area of 117.75 mm<sup>2</sup> the value is 7485.29 N, while the lowest is in elliptical size ratio  $a>b$  (7:3) with an area of 65.94 mm<sup>2</sup> the value is 7429.32 N, for the difference between the highest and lowest value is 55.97 N or 0.7%. The difference in the size of elliptical area with a range from 65.94 mm<sup>2</sup> until 117.75 mm<sup>2</sup> has no significant effect on the average load.

#### 4. Conclusion

Analytical calculations have been carried out on a square tube with 2 elliptical holes on opposite sides with variations in the size of the elliptical ratio of 3:7, 4:6, 5:7.5, 5:6, 6:5, 6:4, 7.5:5, 7 :3 with static axial impact loads, then compared with the simulation results it shows that the difference

between the analytical calculations and the simulation for  $P_{\text{peak}}$  and  $P_{\text{mean}}$  is 3.4% and 3.02% respectively.

The formula for predicting the load from a thin-walled square tube with a static axial impact loads for the prediction of the average load ( $P_{\text{mean}}$ ) is in equation 26, while the  $P_{\text{peak}}$  prediction formula is in equation 27. From the comparison of the analytical calculations and simulations results showed a good conformity.

The influence of the orientation of the a/b ratio and the size of the area on the elliptical hole has a significant effect on the  $P_{\text{peak}}$  value. Where the greater of ratio a/b and the wider of area, so the  $P_{\text{peak}}$  value to be lower.

## Acknowledgments

The author would like to thank the Universitas Indonesia for financial support through the-Hibah PUTI 2022 (Grant No. NKB-335/UN2.RST/HKP.05.00/2022).

## References

- [1] Information on <http://www.bps.go.id/indicator/17/57/1/perkembangan-jumlah-kendaraan-bermotor-menurut-jenis.html> (accessed on August 01, 2023)
- [2] S. Ramakrishna, "Microstructural design of composite materials for crashworthy structural applications," *Materials & Design*, vol. 18, no. 3, pp. 167-173, 1997, doi: [https://doi.org/10.1016/S0261-3069\(97\)00098-8](https://doi.org/10.1016/S0261-3069(97)00098-8).
- [3] A. G. Mamalis, D. E. Manolacos, K. N. Spentzas, M. B. Ioannidis, S. Koutroubakis, and P. K. Kostazos, "The effect of the implementation of circular holes as crush initiators to the crushing characteristics of mild steel square tubes: experimental and numerical simulation," *International Journal of Crashworthiness*, vol. 14, no. 5, pp. 489-501, 2009, doi: <https://doi.org/10.1080/13588260902826547>
- [4] J. I. Felix Dionisius, Tito Endramawan, Irpan J. Sianturi, Suliono, "Pengaruh Crush Initiator Pola Bertingkat terhadap Kriteria Crashworthiness pada Tabung Persegi Berdinding Tipis," *Seminar Nasional Teknologi dan Rekayasa (SENTRA)*, 2017. [Online]. Available: [https://www.researchgate.net/publication/321185199\\_Pengaruh\\_Crush\\_Initiator\\_Pola\\_Bertingkat\\_terhadap\\_Kriteria\\_Crashworthiness\\_pada\\_Tabung\\_Persegi\\_Berdinding\\_Tipis](https://www.researchgate.net/publication/321185199_Pengaruh_Crush_Initiator_Pola_Bertingkat_terhadap_Kriteria_Crashworthiness_pada_Tabung_Persegi_Berdinding_Tipis)
- [5] A. Jusuf, T. Dirgantara, L. Gunawan, and I. S. Putra, "Crashworthiness analysis of multi-cell prismatic structures," *International Journal of Impact Engineering*, vol. 78, pp. 34-50, 2015, doi: <https://doi.org/10.1016/j.ijimpeng.2014.11.011>.
- [6] I. Eren, Y. Gür, and Z. Aksoy, "Finite element analysis of collapse of front side rails with new types of crush initiators," *International Journal of Automotive Technology*, vol. 10, no. 4, pp. 451-457, 2009, doi: <https://doi.org/10.1007/s12239-009-0051-z>
- [7] A. Baroutaji, M. Sajjia, and A.-G. Olabi, "On the crashworthiness performance of thin-walled energy absorbers: Recent advances and future developments," *Thin-Walled Structures*, vol. 118, pp. 137-163, 2017, doi: <https://doi.org/10.1016/j.tws.2017.05.018>.
- [8] G. Sun, T. Pang, J. Fang, G. Li, and Q. Li, "Parameterization of criss-cross configurations for multiobjective crashworthiness optimization," *International Journal of Mechanical Sciences*, vol. 124-125, pp. 145-157, 2017, doi: <https://doi.org/10.1016/j.ijmecsci.2017.02.027>.
- [9] T. Wierzbicki, "Crushing analysis of metal honeycombs," *International Journal of Impact Engineering*, vol. 1, no. 2, pp. 157-174, 1983, doi: [https://doi.org/10.1016/0734-743X\(83\)90004-0](https://doi.org/10.1016/0734-743X(83)90004-0).

- 
- [10] T. Wierzbicki and W. Abramowicz, "On the Crushing Mechanics of Thin-Walled Structures," *Journal of Applied Mechanics*, vol. 50, no. 4a, pp. 727-734, 1983, doi: <https://doi.org/10.1115/1.3167137>
  - [11] W. Abramowicz and N. Jones, "Dynamic axial crushing of square tubes," *International Journal of Impact Engineering*, vol. 2, no. 2, pp. 179-208, 1984, doi: [https://doi.org/10.1016/0734-743X\(84\)90005-8](https://doi.org/10.1016/0734-743X(84)90005-8).
  - [12] A. Niknejad, G. Liaghat, A. H. Behraves, and H. Naeini, "Theoretical Investigation of the Instantaneous Folding Force during the First Fold Creation in a Square Column," *World Academy of Science, Engineering and Technology* vol. 46, 2008.
  - [13] R. J. Hayduk and T. Wierzbicki, "Extensional collapse modes of structural members," *Computers & Structures*, vol. 18, no. 3, pp. 447-458, 1984, doi: [https://doi.org/10.1016/0045-7949\(84\)90065-8](https://doi.org/10.1016/0045-7949(84)90065-8).
  - [14] W. Abramowicz and N. Jones, "Dynamic progressive buckling of circular and square tubes," *International Journal of Impact Engineering*, vol. 4, no. 4, pp. 243-270, 1986, doi: [https://doi.org/10.1016/0734-743X\(86\)90017-5](https://doi.org/10.1016/0734-743X(86)90017-5).
  - [15] W. Abramowicz and T. Wierzbicki, "Axial Crushing of Multicorner Sheet Metal Columns," *Journal of Applied Mechanics*, vol. 56, no. 1, pp. 113-120, 1989, doi: <https://doi.org/10.1115/1.3176030>
  - [16] W. Abramowicz and N. Jones, "Transition from initial global bending to progressive buckling of tubes loaded statically and dynamically," *International Journal of Impact Engineering*, vol. 19, no. 5, pp. 415-437, 1997, doi: [https://doi.org/10.1016/S0734-743X\(96\)00052-8](https://doi.org/10.1016/S0734-743X(96)00052-8).
  - [17] W. Abramowicz, "Thin-walled structures as impact energy absorbers," *Thin-Walled Structures*, vol. 41, no. 2, pp. 91-107, 2003, doi: [https://doi.org/10.1016/S0263-8231\(02\)00082-4](https://doi.org/10.1016/S0263-8231(02)00082-4).
  - [18] C. N. Nguyen, T. Dirgantara, L. Gunawan, I. Putra, and H. Ly, "Analytical Prediction of Square Crash Box Structure With Holes Due To Impact Loading," presented at the Regional Conference on Mechanical and Aerospace Technology, Kuala Lumpur, 2013. [Online]. Available: <http://dx.doi.org/10.13140/2.1.4896.8642>
  - [19] M. Malawat, D.A. Sumarsono, J. Istiyanto, G. Prayogo, and F. Dionisius, "Theoretical prediction of dynamic axial crushing on a square tube with eight holes used as a crush initiator," *Int.J. Technol*, vol. 10, no. 5, pp. 1042-1055, 2019, doi: <https://doi.org/10.14716/ijtech.v10i5.2297>.
  - [20] J. Istiyanto, S. Hakiman, D. A. Sumarsono, G. Kiswanto, A. S. Baskoro, and S. Supriadi, "Experimental and Numerical Study - Effects of Crush Initiators under Quasi-Static Axial Load of Thin Wall Square Tube," *Applied Mechanics and Materials*, vol. 660, pp. 628-632, 2014, doi: <https://doi.org/10.4028/www.scientific.net/AMM.660.628>
  - [21] Y. S. T. M.Y. Huang, H.T. Hu, "Dynamic crushing characteristics of high strength steel cylinders with elliptical geometric discontinuities," *Theoretical and Applied Fracture Mechanics*, vol. 54, pp. 44-53, 2010, doi: <https://doi.org/10.1016/j.tafmec.2010.06.014>
  - [22] Dzikri Amali Musyaffa, Moch. Agus Choiron, Yudy Surya Irawan, Nafisah Arina Hidayati, Taryono Taryono, "Computer simulation investigation of crash box design as safety-protection technology for indonesia high speed train", *International Journal of Mechanical Engineering Technologies and Application*, vol. 4, No. 1, pp. 97 – 103, 2023. DOI: <https://doi.org/10.21776/MECHTA.2023.004.01.11>